Paper Nr: 83

Where Does The Workload Go When Pilots Attack Manoeuvres?

An Analysis Of Results From Flying Qualities Theory And Experiment

by

G D Padfield*   J P Jones+

M T Charlton*   S E Howell*   R Bradley++

* *Defence Research Agency, Bedford*

\+ *Southampton University*

++ *Glasgow Caledonian University*

United Kingdom

TWENTIETH EUROPEAN ROTORCRAFT FORUM

OCTOBER 4 - 7, 1994 AMSTERDAM

Paper Nr: 83

Where Does The Workload Go When Pilots Attack Manoeuvres?

An Analysis Of Results From Flying Qualities Theory And Experiment

by

G D Padfield* J P Jones+

M T Charlton* S E Howell* R Bradley++

* *Defence Research Agency, Bedford*

\+ *Southampton University*

\+\+ *Glasgow Caledonian University*

United Kingdom

CORRECTION

On page 6 in sub - paragraph (vii), expressions are given in parenthesis for the band of values of control attack parameter. These need to be corrected as follows.

$2\omega_\phi/\pi$ should read $\omega_\phi/2$

$4\omega_t/\pi$ should read ωt

G D Padfield

DRA Bedford

Sept 1994

TWENTIETH EUROPEAN ROTORCRAFT FORUM

OCTOBER 4 - 7, 1994 AMSTERDAM

Where Does The Workload Go When Pilots Attack Manoeuvres?

An Analysis of Results from Flying Qualities Theory and Experiment

G D Padfield* J P Jones+

M T Charlton* S E Howell* R Bradley++

Abstract

Analytic simulations have been conducted which show how pilot control strategy is likely to change with the temporal and spatial demands of a mission task element. Theory predicts that the increases in the required control activity can be quite sudden, supporting pilot comments from past flight trials at DRA, that perceived handling can degrade rapidly. Extending this work to numerical simulation of more complex manoeuvres, results show that a critical parameter in the workload assessment is the ratio of aircraft attitude bandwidth to task bandwidth. Frequency and time domain measures of control activity are shown that correlate with this ratio, and indicate where critical values lie. The frequency domain metric investigated is based on the so-called pilot cut-off frequency, defined as the frequency at which 70 % of the control energy has been utilised. An equivalent time domain metric, the so-called attack parameter, is proposed, based on a derivative of the manoeuvre quickness parameter. Each control event can be imagined as a discrete packet of workload and can be extracted from control activity time histories reconstructed as a sequence of attack parameters. Estimating spare (workload) capacity from these metrics is a key research topic and results will be presented for various models of the ideal pilot. The analytic and numerical simulations have led the way to a series of test flights with the DRA Aeromechanics Research Lynx, ALYCAT. Results from a lateral slalom manoeuvre will be presented in detail, showing areas where theory and flight match and also where they begin to break down. Subjective pilot comment, supported by workload metric analysis, provide evidence of where the workload goes when pilot's attack manoeuvres. Finally, the paper discusses how control strategy analysis techniques suggest ways of estimating piloting workload for new mission task elements before flight test data is available. The potential resource savings with such prediction techniques are considerable and serve as a primary motivation for this research.

1 Introduction

Good flying qualities underpin all successful helicopter missions. Spare capacity in terms of aircraft performance and pilot workload go hand in hand with good flying qualities. For safety reasons, pilots generally prefer to fly with performance and workload margins that give sufficient spare capacity for emergencies; this is important for operating with Level 1 handling qualities, according to the Cooper-Harper pilot opinion scale. In life-threatening circumstances however, pilots need to use the full aircraft performance when the piloting task alone will demand full attention. As the demand on agility increases, and by implication pilot workload, so too does the risk of task 'failure' or even flight 'failure' (Ref 1) and key questions concern where the limits to safe operation are for different Mission Task Elements (MTE), and what properties of pilot control activity signal incipient failure. These are questions being addressed in a flying qualities research programme at the DRA Bedford into the correlation of pilot workload with task performance; this paper presents results from this work.

In the paper we are considering a class of operation characterised by the pilot attempting to fly tightly constrained flight paths close to the ground and manoeuvring around obstacles and terrain features. The piloting task can then be divided into two sub-tasks - guidance and stabilisation. Guidance is often referred to as an outer-loop task, concerned with flight path management and maintaining adequate clearance from obstacles, while stabilisation is generally concerned with inner-loop, attitude control. From one point of view these two sub-tasks are complementary - the pilot's cyclic is used both to control the attitude of the aircraft and direct the rotor thrust, generally in harmony. From another point of view there is potential for conflict between the piloting requirements for guidance and stabilisation; afterall, the helicopter pilot only has four controls to control six degrees of freedom. Early research by Neumark at the Royal Aircraft Establishment, into the theory of stability under flight path guidance constraint, identified that fixed-wing aircraft constrained to fly along a prescribed trajectory in the longitudinal plane, could develop attitude/speed instability under certain conditions (Ref 2). In a later paper (Ref 3), Pinsker showed how similar problems could occur in the lateral plane, but this time roll attitude constraint led to a lateral flight path divergence or nose-slice. The problems reported in Refs 2 and 3 were shown by Milne and Padfield in Ref 4 to be limiting cases of pilots applying strong control of one or more aircraft motion variables at the expense of others. The uncontrolled variables, pitch angle in Neumark's work and lateral flight path in Pinsker's, effectively formed into new aircraft modes, the stability of which was threatened under conditions of very strong control by high gain pilots. These examples have demonstrated clearly how requirements for flight path control and attitude stabilisation can conflict and therefore that pilots need to share their workload, shifting priorities as the task demands.

* *Flight Dynamics and Simulation Department, DRA Bedford*

\+ *Southampton University*

++ *Glasgow Caledonian University*

As noted above, helicopter pilots manoeuvring within close physical constraints will normally fly with ample safety margins. However, as the urgency level increases, so flight speeds and levels of pilot aggressiveness on the controls also rise. In these circumstances it is important to understand whether helicopters are susceptible to a loss in stability, in the sense of Refs 2 and 3, or whether the pilot can increase his level of guidance control, or flight path agility, with impunity. In the former case, a key question relates to how the pilot shares his workload between guidance and stabilisation, when a significant degradation in either could lead, in extreme cases, to obstacle strikes or loss of control. Previous flight and simulation research conducted at DRA Bedford (Refs 5, 6) has highlighted the rapid increase in pilot workload with task difficulty; pilot handling qualities ratings (HQR) can degrade from Level 1 to Level 3 with only a modest increase in difficulty beyond a certain level. A key result of this research is that the increase in workload is largely attributed to two main causes - the need for pilots to observe flight envelope limits and degraded response characteristics. The latter can be further divided into two sources - insufficient primary control response and an increase in the level of coupling compensation required; both affect the pilot's ability to contain the guidance and stabilisation tasks and both should be reflected in the patterns of pilot control strategy.

The motivation to be able to identify potential handling problems and to estimate pilot workload through the emerging patterns in pilot control strategy is very strong. For example, the ability to predict workload for new aircraft / MTE combinations without expensive flight trials has obvious attractions. Previous research studies into the estimation of pilot workload for low level helicopter flying tasks (eg Refs 7, 8, 9) have postulated two different frequency ranges of control activity - that associated with the geometry of the flight path (guidance frequency range) and that associated with attitude stabilisation (Ref 8). Condensing this frequency domain perspective of workload, Ref 9 has proposed the so-called pilot 'cut-off frequency' as a workload metric. This parameter is the frequency at which approximately 70 % of the pilot control activity is accounted for, and is illustrated in conceptual form in Fig 1; σ is the root mean square value of the pilot's control signal η. However, while the frequency characteristics are important, they will always tend to blur the spatial and temporal correlation's in a signal, whereas, intuitively, the distribution of energy within a task, particularly one involving a series of transient manoeuvres, will be an important influence on, and indication of, overall pilot workload. A measure of control activity more suited to transient analysis that combines both frequency and amplitude properties can be derived from an extension of the attitude quickness (Refs 1, 10). Fig 2 illustrates the concept, showing how the pilot's control signal can be perceived as a series of discrete fluctuations or commands, each having a change in amplitude and an associated rate of application. A measure of the aggressiveness of control application is given by the ratio of peak rate to control displacement. We call this transient workload metric the attack parameter and hypothesise that levels of workload will appear on the attack charts as shown conceptually in Fig 2 (Refs 11, 12). These transient properties of the control signal can be extracted through the so-called wavelet analysis in the time domain, as opposed to Fourier analysis in the frequency domain. Re-constructing a control signal as a linear combination of wavelets, or worklets, and correlating with the aircraft response, has the potential to enable assessment of the value of individual control actions and to separate the contributions to the guidance and stabilisation sub-tasks (Ref 13). This is a topic of future research.

The paper is organised into three major Sections. Section 2 presents a relatively simple analysis of helicopter behaviour under strong flight path constraints, highlighting the potential problems associated with attitude stability. Section 3 extends this theme with a presentation of results from inverse simulation analysis of slalom flight; here the characteristics of 'ideal' pilot control activity are discussed and workload metrics are derived. Results from preliminary slalom flight tests flown on the DRA Research Lynx, ALYCAT (Aeromechanics Lynx - Control and Agility Testbed), are presented in Section 4. Section 5 contains some concluding remarks. A short Appendix is included that describes some of the features of the numerical scheme used in the inverse simulation package HELINV.

2 Control Strategy in Rolling Manoeuvres - a 2 Dimensional Analysis

To introduce the kind of problem that this paper is addressing we consider a simple model of a helicopter being flown along a prescribed flight path in two-dimensional, horizontal flight. The key points can be made with the most elementary simulation of the helicopter flight dynamics (Ref 14).

A helicopter of mass m and with N_b blades is flying a manoeuvre in the horizontal plane, maintaining height and balance with collective and pedals (Fig 3). Following the usual sign convention for anti-clockwise rotors, the roll angle is ϕ, positive to starboard, and the lateral flapping of the rotor β_{1s}, positive to port. The equation for the rolling moment at the centre of gravity is given by

$$I_{xx}\ddot{\phi} = -M_\beta \beta_{1s} \qquad 1$$

where M_β is the rolling moment per unit flapping given by

$$M_\beta = \left(\frac{N_b K_\beta}{2} + h_R T\right) \qquad 2$$

T is the rotor thrust, which varies during the manoeuvre, h_R is the height of the rotor above the aircraft centre of mass (Fig 3) and I_{xx} is the roll moment of inertia. The hub stiffness K_β can be written in terms of the flap frequency ratio λ_β^2, flap moment of inertia I_β and rotorspeed Ω, in the form

$$K_\beta = \left(\lambda_\beta^2 - 1\right) I_\beta \Omega^2 \qquad 3$$

The equations of force balance in Earth axes can be written

$$T\cos(\phi - \beta_{1s}) = mg \qquad 4$$

$$T\sin(\phi - \beta_{1s}) = m\ddot{y} \qquad 5$$

Combining eqns 1, 4 and 5, and assuming small roll and lateral flapping angles, we obtain the following second order equation for the roll angle ϕ

$$\frac{d^2\phi}{dt^2} + \omega_\phi^2 \phi = \omega_\phi^2 v \qquad 6$$

where v is the normalised side force given in linearised form by

$$v = \ddot{y} / g \qquad 7$$

and the natural frequency ω_ϕ is related to the rotor moment coefficient by the expression

$$\omega_\phi = \sqrt{\frac{M_\beta}{I_{xx}}} = \frac{1}{\sqrt{\tau_\beta \tau_p}} \qquad 8$$

The rotor and fuselage roll time constants are given in terms of more fundamental rotor parameters as

$$\tau_\beta = \frac{16}{\gamma\Omega} \qquad \tau_p = -\frac{1}{L_p} \qquad 9$$

where γ is the rotor Lock number and L_p is the roll damping derivative, which equates to the roll attitude bandwidth for a simple first-order roll model. The small amplitude assumption in eqn 6 implies a constant rotor thrust, hence frequency ω_ϕ. The frequency ω_ϕ is equal to the natural frequency of the roll-flap regressive mode, a combined rotor-fuselage motion with time constant τ_p in free motion.

Equation 6 holds for a general small amplitude lateral manoeuvre and can be used to estimate the rotor forces and moments, hence control activity, required to fly a manoeuvre characterised by the lateral flight path y(t). This represents a simple case of so-called 'inverse simulation', whereby the flight path is prescribed and the equations of motion solved for the loads and controls. A significant difference between rotary and fixed-wing aircraft modelled in this way is that the inertia term in eqn 6 vanishes for fixed-wing aircraft, with the sideforce then being simply proportional to the roll angle. For helicopters, the loose coupling between rotor and fuselage leads to the presence of a mode with frequency ω_ϕ, as given by eqn 6, representing an oscillation of the aircraft relative to the rotor, while the rotor maintains the prescribed orientation in space. Motion of the fuselage in this mode therefore has no effect on the flight path of the aircraft. It should be noted that this 'mode' is not a feature of unconstrained flight, where the two natural modes (assuming quasi-steady rotor motion) are a roll subsidence (magnitude L_p) and a neutral mode (magnitude 0) representing the indifference of the aircraft dynamics to heading or lateral position. The degree of excitation of the 'new' mode depends upon the frequency content of the flight path excursions and hence the sideforce v. For example, when the prescribed flight paths are genuinely orthogonal to the mode (ie combinations of sine waves), then the response of the latter will be zero. In practice, slalom - type manoeuvres, while similar in character to sine waves, can have significantly different load requirements at the turning points, and the scope for excitation of the unconstrained mode is potentially high. A further important point to note about the character of the solution to eqn 6 is that as the frequency of the flight path approaches *the natural frequency ω_ϕ, then the roll angle response approaches resonance.* To understand what happens in practice, we must look at the equation for 'forward' rather than 'inverse' simulation. This can be written in terms of the lateral cyclic control input θ_{1c} forcing the flight path sideforce v, in the approximate form

$$\frac{d^2 v}{dt^2} - L_p \frac{dv}{dt} = \left\{ \frac{d^2\theta_{1c}}{dt^2} + \omega_\phi^2 \theta_{1c} \right\} \qquad 10$$

The derivation of this equation has assumed that the rotor responds to control action and fuselage angular rate in a quasi-steady manner, taking up a new disc tilt instantaneously. In reality the rotor responds with a time constant τ_p, but for the purposes of the present discussion, this delay will be neglected. The presence of the control acceleration term on the right hand side of eqn 10 is critical to what happens close to the natural frequency. In the limit, when the input frequency is at the natural frequency, the flight path response is zero due to the cancelling of the control terms, hence the theoretical artefact in eqn 6, that the roll angle would grow unbounded at that frequency. As the pilot moves his stick at the critical frequency, the rotor disc remains horizontal and the fuselage wobbles beneath. For cyclic control inputs at slightly lower frequencies, the side forces are still very small and large control displacements are required to generate the turning moments. Stick movements at frequencies higher than ω_ϕ produce small forces of the opposite sign, acting in the wrong direction. Hence, despite intense stick activity the pilot may not be able to fly the desired track. The difference between what the pilot can do and what he is trying to do, increases sharply with the severity of the desired manoeuvre and the upper limit to what can usefully or safely be accomplished, in terms of task bandwidth, is determined by the frequency ω_ϕ (Ref 14). For current helicopters, the natural frequency varies from about 6 rad/sec for low hinge offset, slowly rotating rotors, to 12 rad/sec, for hingeless rotors with higher rotor speeds. Fig 4 illustrates the solution to the inverse form of eqn 10 for two different helicopters flying a lateral slalom 300m in length and 30m wide at 30m/sec (approx. 60 kn). In Fig 4, the lateral cyclic is plotted against manoeuvre distance. The two cases correspond to a relatively stiff rotor with moderately high rotor speed (equivalent offset 13 %, Ω = 35 rad/sec), and an articulated rotor at fairly low rotor speed (offset 5 %, Ω = 25 rad/sec). The helicopter with the softer rotor requires 40 % greater control inputs and the control activity is contaminated by the response to the unconstrained mode.

The preceding analysis is based on small amplitude perturbations about a straight and level trim condition. The qualitative nature of the results do not change significantly for large manoeuvres. The response amplitude and phase still change rapidly as some critical frequency is approached and the 'free' attitude mode is subject to the same excitation governed by the shape of the flight path. Nonlinearities due to thrust variations and track curvature will affectfrequencies and amplitudes however, but these are difficult to predict analytically. We shall gain some appreciation of these effects in the next Section when discussing results from nonlinear inverse simulation.

Two questions arise out of the above simple analysis that are relevant to understanding the impact on pilot workload. First, as the task bandwidth increases, what determines the limiting frequency, beyond which control activity becomes *unreasonably high and how can this frequency be predicted ?* Second, how does the pilot cope with the unconstrained oscillations, if indeed they manifest themselves in practice; while these oscillations have little or no effect on the flight path, the pilot will almost certainly try to neutralise them to improve ride quality. A useful parameter in the context of these questions is the ratio of aircraft to task natural frequencies. The task natural frequency ω_t can, in general, be derived from a frequency analysis of the flight path variations but, for simple slalom manoeuvres, the value is approximately related to the inverse of the task time. It is suggested in Ref 14 that a meaningful upper limit to task frequency can be written in the form

$$\frac{\omega_\varphi}{\omega_t} > 2\, n_v \qquad 11$$

where n_v is the number of flight path changes required in a given task. A two-sided slalom for example, as illustrated in Fig 5, contains 5 such distinct changes, hence at a minimum, for slalom manoeuvres

$$\frac{\omega_\varphi}{\omega_t} > 10; \qquad \frac{\omega_\varphi}{10\,\omega_t} > 1 \qquad 12$$

This suggests that a pilot flying a reasonably agile aircraft with an ω_ϕ of 12 rad/s could be expected to experience control problems when trying to fly any two-sided slalom in less than about 5 seconds. A pilot flying a less agile aircraft (ω_ϕ = 6 rad/s) might experience similar control problems in a 10 second slalom. This 100% increase in usable performance for an agile helicopter clearly has very important implications for military and some civil operations and needs to be tested in practice. Before presenting flight test results, a more general analysis of inverse simulation will be presented.

3 Compensatory Workload in Aggressive Manoeuvres - Inverse Simulation Predictions

The development of inverse simulation for application to helicopter flight dynamics has been reported extensively in the literature, particularly at European Rotorcraft Fora; we refer to the work of Thomson and Bradley and the inverse simulation package HELINV in this Section, as described in Refs 12, 15 and 16. One of the features of the numerical technique employed in such inverse solutions to dynamic problems is the effect of the integration time interval on the damping of the 'free' oscillation. The Appendix to this paper discusses this effect. The simple concepts outlined in Section 2 can be generalised for six degree of freedom helicopter motion. For manoeuvres in the horizontal plane we elect to constrain aircraft height, speed, sideslip and lateral ground track. This is the limit to the number of states that can be prescribed with only four controls and our main interest is with variations in lateral ground track and the consequent impact on lateral cyclic required. We can write the prescribed lateral flight path as a polynomial in time

$$y(t) = y_{max} \sum_{k=0}^{N} \alpha_k \left(\frac{t}{t_1}\right)^k \qquad 13$$

where y_{max} is the maximum extent of the flight path excursions and the α_k coefficients are defined for particular manoeuvres; t_1 is a normalising time. A more typical definition of a manoeuvre for pilots to fly is provided by the descriptions of the flight test manoeuvres in ADS33C (Ref 10); for the aggressive slalom the manoeuvre description reads,

Initiate the manoeuvre in level unaccelerated flight and lined up with the centreline of the test course. Perform a series of smooth turns at 152m (500 ft) intervals. The turns shall be at least 15.2 m (50 ft) from the centreline, with a maximum lateral error of 15.2m. The manoeuvre is to be accomplished at a reference altitude below 30.5 m (100 ft). Complete the manoeuvre on the centreline. Maintain an airspeed of at least 60 kn (desired), or 40 kn (adequate), throughout the course.

Flying this ADS manoeuvre in inverse simulation terms requires interpreting the limited number of defined constraints in terms of the boundary conditions on eqn 13. The minimum number of conditions that give a two-turn slalom is ten, as follows;

$$\begin{array}{lllll} \text{i)} & t = 0, & y = 0, & \dot{y} = 0, & \ddot{y} = 0 \\ \text{ii)} & t = t_1, & y = y_{max}, & \dot{y} = 0 & \\ \text{iii)} & t = 2t_1, & y = -y_{max}, & \dot{y} = 0 & \\ \text{iv)} & t = 3t_1, & y = 0, & \dot{y} = 0, & \ddot{y} = 0 \end{array} \qquad 14$$

The requirement for zero acceleration at t = 0 ensures that the pilots cyclic only starts moving at the beginning of the slalom. The time t_1 is set at 1/3 the manoeuvre duration and y_{max} is the minimum ADS lateral displacement of 15.2m. The coefficients of eqn 13 then become

$$\alpha_9 = -0.125, \alpha_8 = 1.688, \alpha_7 = -9.0, \alpha_6 = 23.63,$$
$$\alpha_5 = -30.38, \alpha_4 = 15.19, \alpha_3 = \alpha_2 = \alpha_1 = \alpha_0 = 0.0 \qquad 15$$

We define the aspect ratio (AR) of the slalom as the ratio of width to length. Fig 6 illustrates examples of the HELINV slalom for ARs of 0.04, 0.08 and 0.12; the ADS33C minimum slalom, 100 ft wide and 1500 ft long, results in an AR = 0.067. Variations in the two key frequency parameters, ω_ϕ and ω_t, can be made through the rotor system flapping stiffness (K_β in eqn 2) and slalom aspect ratio AR. Flight speed is also a discriminating parameter, but for the most part we shall be discussing the 60 kn slalom case. The results of a detailed HELINV analysis of control activity in ADS33C slaloms are presented in Figs 7 - 12 and summarised in the following paragraphs.

(i) Fig 7 shows the linear variation of agility factor (Refs 1, 5) with forward speed. The agility factor is the ratio of the ideal manoeuvre time to the actual manoeuvre time (distance flown/speed). The ideal manoeuvre time is calculated assuming flight at constant speed along straight segments between the offset slalom poles. The three cases shown correspond to the limiting speeds achieved with Lynx fitted with three different rotor systems - hingeless, articulated and teetering flap retention. The limiting speed in all cases corresponds to the lateral cyclic reaching the control stops. With the teetering rotor as the baseline, Fig 7 suggests a 25 % increase in flight speed achievable with the articulated rotor and nearly 40 % increase with the hingeless rotor, for aircraft with the same cyclic control range.

(ii) Fig 8 shows a comparison of the roll attitude (Fig 8a) and rate (Fig 8b) responses for the same three aircraft of Fig 7, but all flown at the limiting AR (AR = 0.077) for the teetering rotor at a slalom speed of 60 kn. The attitude changes, not surprisingly, are very similar for the three cases, as are the rates, although we can now perceive the presence of higher frequency motion in the signal for the teetering and articulated rotors. For the teetering rotor, roll rate peaks some 20 - 30% higher than found with the hingeless rotor can be observed, entirely a result of the component of the free mode in the aircraft response.

(iii) Fig 9a illustrates the lateral cyclic required to fly the manoeuvre of Fig 8. The difference between the three rotor configurations is now very striking. The Lynx, with its standard hingeless rotor, requires 30 % of maximum control throw, while the articulated rotor requires slightly more at about 35 %. The extent of the excitation of the free oscillation for the three configurations can be clearly seen in the time histories of Fig 9a, but are better quantified in the lateral cyclic auto spectra in Fig 9b. The control activity in all three cases share the component associated with the task bandwidth at about 1 rad/sec. With the teetering rotor however, the control required to fly the task has much stronger higher frequency components with a second dominant peak centred around the roll / flap mode natural frequency ω_ϕ ($\approx$ 4.5 rad/sec). We distinguish between these two components of control activity. The lower frequency component is the minimum required to manoeuvre the aircraft around the course and we describe this as the guidance component. The higher frequency component has no effect on the flight path and is described as the stabilisation component. One important observation is that the frequency of the guidance control is approximately twice the task frequency. This is a result of the rate-command nature of roll control on the Lynx, so that for every flight path change, two distinct control inputs are required.

(iv) The variation of maximum lateral cyclic with AR used by Lynx in the slalom, typically during the roll reversal, is shown in Fig 10. The Lynx appears to be unable to fly the slalom at an aspect ratio above about 0.11, corresponding to an ω_t of 0.7 rad/sec (T $\approx$ 10 sec) and a value of $\omega_\phi/10\omega_t$ of about 2. At this condition the HELINV pilot runs out of lateral cyclic during the acquisition phases of the slalom. The criterion in eqn 12 suggests that, if the pilot had more control authority, then the HELINV Lynx could be flown up to an aspect ratio of 0.2 without significant control problems.

(v) The lateral cyclic pilot cut-off frequency, as described in Section 1, is shown as a function of $\omega_\phi/10\omega_t$ for various values of AR and rotor stiffness in Fig 11; the flight speed for all cases is 60 kn. Four different rotor stiffnesses are shown on the Figure. The stiffness factor of unity corresponds to the Lynx, with an ω_ϕ of approximately 12 rad/sec. The stiffness factor of 0.75 corresponds to typical current generation hingeless rotors (with effective flap hinge offsets of about 10 %). A stiffness factor of 0.25 simulates a typical articulated rotor with about 4 % flap hinge offset, while a zero stiffness corresponds to a teetering rotor. The maximum AR / cut-off frequency reached with each rotor system corresponds to the lateral cyclic reaching the control stops. For both the higher stiffness configurations, the 'workload' trend with the bandwidth ratio has a hyperbolic form - the workload is almost entirely guidance-centred up to the control limit, so that ω_{co} varies as the inverse of ω_t. For the teetering rotor, and to lesser extent the articulated rotor, the workload increases dramatically as the AR is increased and is dominated by the stabilisation component above an AR of 0.05. The upper boundary on Fig 11 defines the limiting aspect ratio for each rotor. For example, at an AR of about 0.07, the hingeless and articulated rotors have significant spare capacity, both in terms of control margin and margin from the critical value of $\omega_\phi/10\omega_t$. The teetering rotor on the other hand has hit both the control limit and the critical bandwidth ratio at this AR. The data on Fig 11 suggests that the limiting bandwidth ratio should actually be rather higher than suggested by the intuitive reasoning that led to eqn 12; a critical value of $\omega_\phi/10\omega_t$ of 1.5 appears to be more appropriate.

(vi) We can deduce from the previous results that the pilot cut-off frequency gives a clear indication of the level of control activity workload in a mission task element. The relationship can be conceptually represented as shown in Fig 12, which should hold for a range of lateral manoeuvres. The two boundaries on Fig 12 correspond to limiting guidance and stabilisation workload. The relative proportions of the guidance and stabilisation workload in a particular case will depend on a number of factors. The lower the bandwidth ratio, then the higher will the proportion of stabilisation to guidance workload. The hashed boundary lines on Fig 12 represent the suggested performance limits - the upper boundary set by available control margin, the vertical boundary setting an acceptable limit to the ratio of stabilisation to guidance workload. The cusp of the two workload contours corresponds to the case when the workload is purely guidance, giving a value of ω_{co} of $2\omega_t$.

(vii) Finally in this series of HELINV results, Figs 13a and 13b show the attitude quickness ($p_{pk}/\Delta\phi$) and cyclic attack ($\dot{\eta}_{1c_{pk}} / \Delta\eta_{1c}$) charts for the slalom runs, again for the three different rotor systems. The ADS33C Level 1/2 and 2/3 boundaries for attitude quickness are also drawn. The quickness points practically all lie below the Level 2/3 boundary, but for the hingeless and articulated rotors this simply says that higher values of quickness were not required to perform the task. The teetering rotor configuration, on the other hand, is using maximum attitude quickness to just fly the slalom, indicating, at best, poor Level 2 handling qualities. The lateral cyclic attack chart shown in Fig 13b has several interesting features. The 100 % /sec control rate boundary is also drawn, noting that the control range is between $-1 < \eta_{1c} < 1$; for the HELINV flights there was no restriction on control rate. Each value of attack corresponds to a discrete pilot - commanded flight path change or attitude correction. The highest attack values, shown boxed in the Figure, occur after the initial roll into the slalom. The value corresponding to the teetering rotor reaching the control limits during the roll reversals is also highlighted. The clearly defined band of attack values for the teetering configuration relates to the control inputs at the 'free' oscillation, with values grouped around 2.5 rad/sec (ie $2\omega_\phi/\pi$). In contrast, the attack values for the articulated and hingeless rotor configurations have groupings between 0.5 and 1, corresponding to the task frequency (ie $4\omega_t/\pi$). Based solely on the number of attack points, there is three times the control activity with the teetering rotor compared with the hingeless rotor and twice as much compared with the articulated - measures which correlate with the different levels of ω_{co}. seen in Fig 11. Quality is even more important than quantity, however, and it should also be apparent that most of the attack values for the teetering rotor are fairly unproductive as far as the guidance task is concerned. Workload boundaries on the attack chart correspond to dynamic control margins, taking an approximately hyperbolic shape at moderate to large amplitude. We shall return to discuss this issue further in relation to the flight results.

Before we discuss the related results from the flight trials, it is useful to summarise the HELINV predictions for Lynx. *Up to the limiting AR of about 0.11, the HELINV Lynx can be flown with an essentially guidance control strategy*, with a pilot cut-off frequency of approximately twice the task bandwidth, ie $\approx$ 1.5 rad/sec. The corresponding bandwidth ratio ($\omega_\phi/10\omega_t$) at this condition is about 1.8, which is relatively close to the critical ratio of 1.5 postulated from the HELINV results. The attack chart shows a relatively small number of discrete control inputs, with a significant margin across the full amplitude range.

The simulation model internal to HELINV is based on the DRA Helisim model, where the rotor is treated as a disc with multi-blade co-ordinate flapping degrees of freedom. In this study we are more concerned with achieving the correct trends between flight and theory, rather than with high fidelity. In support of this requirement, Figs 14a and 14b show a comparison of lateral cyclic for HELINV and real Lynx flying the 10 % slalom (AR = 0.1). The data are shown as a cross plot against roll rate, highlighting the essentially rate command character of both simulation and test response-type. While the HELINV control activity clearly contains far fewer reversals than the flight test data, the overall character is similar. Rate sensitivity for the test data appears some 20 % less than HELINV, eg control power is estimated from extrapolation to be about 90 deg/sec in flight and about 110 deg/sec in HELINV. However, the HELINV results are derived from blade angles, while the test data are derived from stick position; the actuation system will introduce a time lag and modify the simulation data to give an even closer resemblance with the test data.

4 How Does the Pilot Compensate in Flight ? - Results from Alycat Lynx Trial

In this Section we describe results from a preliminary flight trial to test the various hypotheses proposed in Sections 2 and 3. The DRA research Lynx ALYCAT was flown in a series of slaloms marked out on the runway with traffic cones defining the ground track. Slalom aspect ratios from 0.03 to 0.12 were defined by fixing the lateral offset of the cones at 15.2m from the centreline and varying the length of the course. The course flown was a slight variation on the HELINV ADS33C slalom as shown in Fig 15, with the offset cones at the 1/4 and 3/4 points compared with the 1/3 and 2/3 points for the ADS slalom. Some 4 - 5 runs were flown at each AR. The desired (adequate) task performance requirements were set at ,

track at turning points ± 3 (6) m;   height ± 3 (4.5) m;   speed ± 5 (7.5) kn

The human pilot will differ from the HELINV pilot in a number of respects. A greater anticipatory control strategy will be used and, unlike the HELINV pilot, the human pilot will incur task performance errors. The human pilot will also need to use a more complex control strategy to compensate for cross couplings, atmospheric disturbances (including the effects of steady winds), sideslip excursions and to correct for any errors of judgement. Nevertheless, we can expect the primary demands on lateral cyclic to mirror those in HELINV reasonably faithfully.

The results from the flight trials are presented in Figs 16 - 22 and summarised in the following paragraphs.

(i) Fig 16 shows sample time histories of lateral cyclic, roll rate and roll attitude for the AR = 0.06, 0.08, 0.1 and 0.12 cases. The corresponding handling qualities ratings (HQR) are 4, 4, 5.5 and 6. For the AR = 0.12 runs, the pilot was commanding full lateral cyclic control on occasions, with bank angles in excess of 60 deg and roll rates approaching 80 deg/sec; he returned borderline Level 2/3 HQRs for this AR, the highest that he was prepared to fly. In the event, the task performance for this AR, in terms of speed and track error, fell outside the adequate boundary, hence the HQRs should strictly be corrected into the Level 3 region.

(ii) For slaloms with ARs of 0.08 and above, the lateral cyclic and associated roll rate response contain distinct high frequency components. Fig 17 shows a comparison of lateral cyclic power spectrum for the smallest and largest AR cases. The activity in the guidance frequency range has increased by an order of magnitude at the upper AR limit, but it is the activity in the stabilisation band, from 1 - 2.5 Hz, that is the major distinguishing feature between the two cases.

(iii) A comparison of the pilot cut-off frequency estimated from the HELINV runs and flight tests is shown in Fig 18. The flight data appears shifted to the right relative to the HELINV results, an effect caused by the longer flight task times. The pilot tended to fly outside the offset poles and hence a longer overall track. Also at the larger aspect ratios, the pilot was unable to hold the task speed within the adequate performance margins, with excursions falling below 50 kn on occasions. Taking this scaling correction into account the agreement between HELINV and Flight is very good. In the flight situation, the pilot returned poor Level 2 ratings at the highest AR values, downgraded to Level 3 after the event because of failure to achieve the task.

(iv) The transient properties of the flight results are presented in Figs 19 - 22. Attitude quickness and lateral cyclic attack for the AR = 0.08 case are shown in Figs 19a and 19b respectively; the HELINV data for the AR=0.077 case already discussed are included on the charts for comparison. The five attack values for the HELINV flight correspond to the simple guidance control strategy commanding the flight path changes. The pilot flying the slalom makes over 30 distinct attacks during this 15 second slalom, shown as a function of manoeuvre time in Fig 20. During the roll reversals the pilot typically makes 10 commands, each corresponding to an attack value, compared with a single command used by the HELINV pilot. Practically all of the control inputs made by this pilot have associated attack values greater than 2; effectively, the low frequency guidance strategy adopted by the HELINV pilot is broken down into a larger number of higher frequency stabilisation commands, overlaid on the guidance strategy. There appears to be no obvious way of determining the effectiveness of these control inputs, which have a stronger content at the natural roll frequency ω_ϕ as the AR increases. The upper limits on measured attack for the Lynx flying the different AR slaloms are shown on Fig 21. As pointed out earlier, for the AR = 0.12 case the pilot failed to achieve the adequate task performance level, hence his return of HQR 6 should be downgraded to Level 3. At the other extreme, the AR = 0.04 case was returned an HQR 3 rating, ie close to the Level 1/2 boundary. Based on these tentative observations, Fig 22 illustrates suggested workload boundaries on the attack chart. The Level 1, AR = 0.04 points are included for reference.

The synthesis of pilot control activity as transient or periodic commands provides a framework for a rational analysis of workload in terms of guidance and stabilisation control strategies. The two approaches are complementary and both enable comparisons between aircraft to be made. HELINV simulations have provided a remarkably reliable indication of the maximum performance capability of Lynx flying lateral slaloms, with an aspect ratio of about 0.11 achievable before lateral cyclic control limits are reached. The increased guidance and stabilisation demands on the pilot workload, as slalom task bandwidth is increased, is reflected in both the pilot cut-off frequency and control attack parameters. The control attack provides additional insight into the spatial and temporal distribution of workload and future research efforts will be focused on this area in particular. One avenue receiving attention currently is the use of wavelet analysis to decompose the control action into a combination of worklets, each having an associated amplitude and time scale (Refs 12, 13). Each worklet also has its own unique attack signature, and this property suggests a systematic approach to the derivation of both attack and quickness parameters. Control activity can be re-constituted into guidance and stabilisation components, effectively providing a method for establishing the productivity of each control movement.

Looking to the application of control workload measurement, there are several potentially fruitful avenues. For example, HELINV analysis offers the opportunity to determine the capability of a helicopter to fly new MTEs, or a new design to fly the ADS33C MTEs. Alternatively, the desired handling characteristics for achieving Level 1 performance in new MTEs can be established. In this context, inverse simulation can currently be used to derive an initial estimate of the performance limits of a new configuration. The capability for on-line measurement and prediction of workload during flight test is also suggested by the research in this paper. In the evaluation of new piloting aids, engineering workload metrics can be an invaluable support to clarifying and interpreting subjective pilot comment, alongside the objective measurement of task performance. Further research is needed to ensure that the techniques outlined in this paper have the robust properties needed for routine use with a wider range of MTEs. The examples discussed have only considered the influence of primary control activity (lateral cyclic in the slalom) on workload. The techniques could be extended to include the effects of compensatory inputs in other control axes, or to cases where two or more axes of control have a primary role. The influence of atmospheric disturbance will also need to be accounted for; clearly, they can have a potentially significant effect on workload, especially when the disturbance spectrum, or range of attitude quickness caused by the disturbances, spans both the guidance and stabilisation bands.

5 Conclusions

This paper has reported results of a DRA research programme aimed at developing engineering metrics for the prediction of pilot workload. The metrics evaluated are derived from frequency and time domain analysis of pilot control activity. The key premise of this work is that when pilots are attempting to fly a tightly constrained flight path, for example in low level flight around obstacles, the workload divides into two increasingly conflicting requirements - guidance and stabilisation. A historical perspective on this problem has been provided by reference to early fixed-wing work on the stability of aircraft under constraint. Two-dimensional flight mechanics theory has been shown to predict that the stability of the helicopter attitude motion is degraded under the influence of strong flight path control. The fundamental frequency of the so-called 'free' oscillation, ω_ϕ, has been related to the natural frequency of the coupled body roll / rotor flap mode. A key parameter that appears to determine the extent of control activity, and hence task workload, is the ratio $\omega_\phi/(n_v\omega_t)$, where ω_t is the task bandwidth (closely approximated by $2\pi/T$ for the slalom MTE) and n_v is the number of flight path changes in the mission task element. In an attempt to understand the implications for accurate low level flying tasks, results from inverse simulations (using the HELINV inverse simulation software) and flight tests with Lynx flying a lateral slalom course have been analysed and compared. The slalom difficulty was increased by increasing the ratio of slalom width to length - the aspect ratio AR. From the results presented the following observations can be made and conclusions drawn.

(i) From the HELINV analysis we observe that the character of the lateral cyclic control activity changes dramatically for $\omega_\phi/(n_v\omega_t)$ ratios lower than about 1.5, with the residual, and unproductive, high frequency control activity dominating and obscuring the lower frequency guidance control. Increasing ω_ϕ through rotor stiffness allows increasingly more performance to be achieved in the slalom, measured either in terms of higher speeds or increased AR. The standard Lynx configuration can successfully negotiate the slalom course up to an AR of about 0.11, with an essentially guidance strategy, at which point the lateral cyclic reaches the control stops.

(ii) Analysis of the pilot cut-off frequency ω_{c0} from the HELINV results provides a clear indication of the changing character in the control activity as the task demands increase. For the low stiffness rotors, ω_{c0} increases two to three fold as the bandwidth ratio reduces below the critical value. For the HELINV Lynx flying its maximum slalom AR, ω_{c0} is accounted for almost entirely with guidance control strategy.

(iii) The control attack parameter provides information on the distribution of control inputs, hence workload, as a function of (time) scale and amplitude. Spare capacity is intuitively related to the dynamic control margin on these attack parameter charts.

(iv) Comparison between flight and simulation for the pilot cut-off frequency metric shows good agreement, with both 'cutting-off' at about 1.5 rad/sec at the limiting AR of about 0.11. In flight, the pilot returned poor Level 2 HQRs in this condition.

(v) Comparison between flight and simulation for the transient attack parameter has revealed considerably more control activity in flight than with the 'perfect' HELINV pilot. Typically a single HELINV control action compares with between 5 and 10 by the flight pilot. Boundaries on the attack charts have been proposed that distinguish between workload demands corresponding to Level 1, 2 and 3 handling qualities.

Areas for future research and applications of the use of engineering workload metrics have been suggested, some of which are ongoing. One of the most promising involves the decomposition of the pilot's control activity into single actions, described as worklets, utilising the wavelet transform. Analysis of the temporal distribution of worklets suggests a natural decomposition into guidance and stabilisation components, from which the productivity of individual pilot control movements can be determined.

References

1 Padfield, G.D., Hodgkinson, J., The Influence of Flying Qualities on Operational Agility, AGARD CP 548, Technologies for Highly Manoeuvrable Aircraft', March 1994

2 Neumark, S., Problems of Longitudinal Stability below Minimum Drag Speed and Theory of Stability Under Constraint, ARC R&M 2983, 1957

3 Pinsker, W.J.G., Directional Stability in Flight With Bank Angle Constraint as a Condition Defining a Minimum Acceptable Value for Nv, RAE Tech Report 67 127, June 1867

4 Milne, R.D., Padfield, G.D., The Strongly Controlled Aircraft, The Aeronautical Quarterly, Volume XXII, Part 2, May 1971

5 Charlton, M.T., Padfield, G.D., Horton, R., Helicopter Agility in Low Speed Manoeuvres; Proceedings of the 13th European Rotorcraft Forum, Arles, France, Sept 1987 (also RAE TM FM22, 1989)

6 Padfield, G.D., Charlton, M.T., Kimberley, A.K., Helicopter Flying Qualities in Critical Mission Task Elements; Initial Experience with the DRA Bedford Large Motion Simulator, 18th European Rotorcraft Forum, Avignon, France, Sept 1992

7 Pausder, H.-J., Hummes, D., Flight Tests for the Assessment of Task Performance and Control Activity, J. American Helicopter Society, Vol 29, No 2, 1984

8 Padfield, G.D. Charlton, M.T., Houston, S.S., Pausder, H.-J., Hummes, D., Observations of Pilot Control Strategy in Low Level Helicopter Flying Tasks, Vertica, Vol 12, No 3, 1988

9 Pausder, H.-J., Blanken, C.L., Investigation of the Effects of Bandwidth and Time Delay on Helicopter Roll Axis handling Qualities, Piloting Vertical Flight Aircraft - A Conference on Flying Qualities and Human Factors, NASA/AHS Specialists Meeting, San Fransisco, Jan 1993

10 Anon., Aeronautical Design Standard 33C, Handling Qualities Requirements for Military Rotorcraft, US Army Aviation Systems Command, St Louis, Mo., August 1989

11 Charlton, M.T., Houston, S.S., Flight Test and Analysis Procedures for New Handling Criteria, RAeSoc. Conference on Helicopter handling Qualities and Control, London, Nov 1988

12 Thomson, D.G., Bradley, R., The Contribution of Inverse Simulation to the Assessment of Helicopter Handling Qualities, Proc. 19th ICAS Conference, Anahiem, Sept 1994

13 Jones, J.G., Turner, G.P., Application of Adaptive Wavelet Analysis to the Assessment of Helicopter Agility, DRA Working Paper AS/FS/WP 93040/1, Sept 1993

14 Jones, J.P., Notes on Helicopter Agility, Private Communications, 1993/4

15 Thomson, D.G., Bradley, R., The Use of Inverse Simulation for Conceptual Design, 16th European Rotorcraft Forum, Glasgow, Sept 1990

16 Thomson, D.G., Bradley, R., Prediction of the Dynamic Characteristics of Helicopters in Constrained Flight, The Aeronautical Journal, Dec 1990

Acknowledgements

This work was conducted under the UK MoD's Strategic Research Programme, item AS021W14 - Correlation of Pilot Workload with Flying Qualities and Task Performance. The authors would like to acknowledge the contribution made by the DRA (Bedford) rotary wing test test pilot, Lt Cdr Steve Cheyne, to this work. Support with the HELINV analysis was provided by Dr Doug Thomson at Glasgow University. This research forms an element of an on-going tri-partite collaborative programme into helicopter handling qualities between the DRA Bedford, DLR Braunschweig and US Army Aeroflightdynamics Directorate involving complementary use of the AFS and VMS ground-based simulation facilities, the research Lynx and Blackhawk and the DLR's fly-by-wire Bo105, ATTHeS.

Appendix

Sensitivity of 'Free Oscillations' to Integration Time Step

The lightly damped, or even unstable, modes that can arise out of the constrained dynamics of inverse simulation have been reported by Thomson and Bradley in Ref 16. This Appendix addresses the observed sensitivity of the damping of these modes to integration step in the simulation process. In order to provide an explanation of this effect, the equations of linear analysis are recalled from the main text. The response in roll angle to prescribed lateral flight path acceleration is given by

$$\frac{d^2\phi}{dt^2} + \omega_\phi^2\phi = \omega_\phi^2 v \qquad \text{A1}$$

and the lateral flapping is given by

$$\beta_{1s} = \phi - \upsilon \qquad \text{A2}$$

In the HELINV package, an implicit numerical method using backward differences is employed for solving the equations of motion. Implicit methods are well known for their beneficial properties as regards numerical stability, and in general terms it is this property that explains the observed phenomena when using HELINV. Applied to the roll dynamics problem above, the implicit method can be cast in the discrete form

$$\left(\phi_n - 2\phi_{n-1} + \phi_{n-2}\right) / h^2 + \omega_\phi^2\phi_n = \upsilon_n \qquad \text{A3}$$

where the suffix n is the index of the time step and h is the step length. The complementary function of this difference equation is governed by the relation

$$\left(1 + h^2\omega_\phi^2\right)\lambda^2 - 2\lambda + 1 = 0 \qquad \text{A4}$$

so that the transient response is defined by the parameter

$$\lambda = \frac{1 \pm ih\omega_\phi}{1 + h^2\omega_\phi^2} \qquad \text{A5}$$

Since $|\lambda|<1$ it is clear that transients decay with time and for $h\omega_\phi < 1$, the discrete form above has transients that decay like a second order system with damping factor

$$\zeta \approx \frac{h\omega_\phi}{2} \qquad \text{A6}$$

The control of the effective damping through the step length, h, is clear. For example, with ω_ϕ in the range 7 - 12 rad/sec, and h = 0.1, the damping factor is estimated to lie in the range 0.35 - 0.6. In several of the published papers showing HELINV results, the interest was focused on the main trends of the control activity so that the suppression of the transients through an appropriate choice of h was beneficial. In the present study, the extent of the transients in the 'free' mode are significant for workload analysis and more care must be taken. Fig A1 shows a typical result from the above equations for a soft rotor, with ω_ϕ = 6 rad/sec; three case of time step are shown. The largest time step (note that no numerical instability has occurred) of 0.1 entirely suppresses the oscillations, while an h of 0.001 recovers the full extent of the almost undamped oscillation. The frequency of the oscillation remains independent of the time step, at ω_ϕ. It is emphasised that this lateral cyclic input has no effect on the flight path but causes the aircraft to rock under the rotor. A question that arises out of this analysis concerns whether a pilot would ever bother to close the loop on aircraft attitude at this frequency. The roll attitude will certainly be excited at this frequency by certain flight path characteristics and it is suspected that pilot intervention will require considerable skill to be effective.

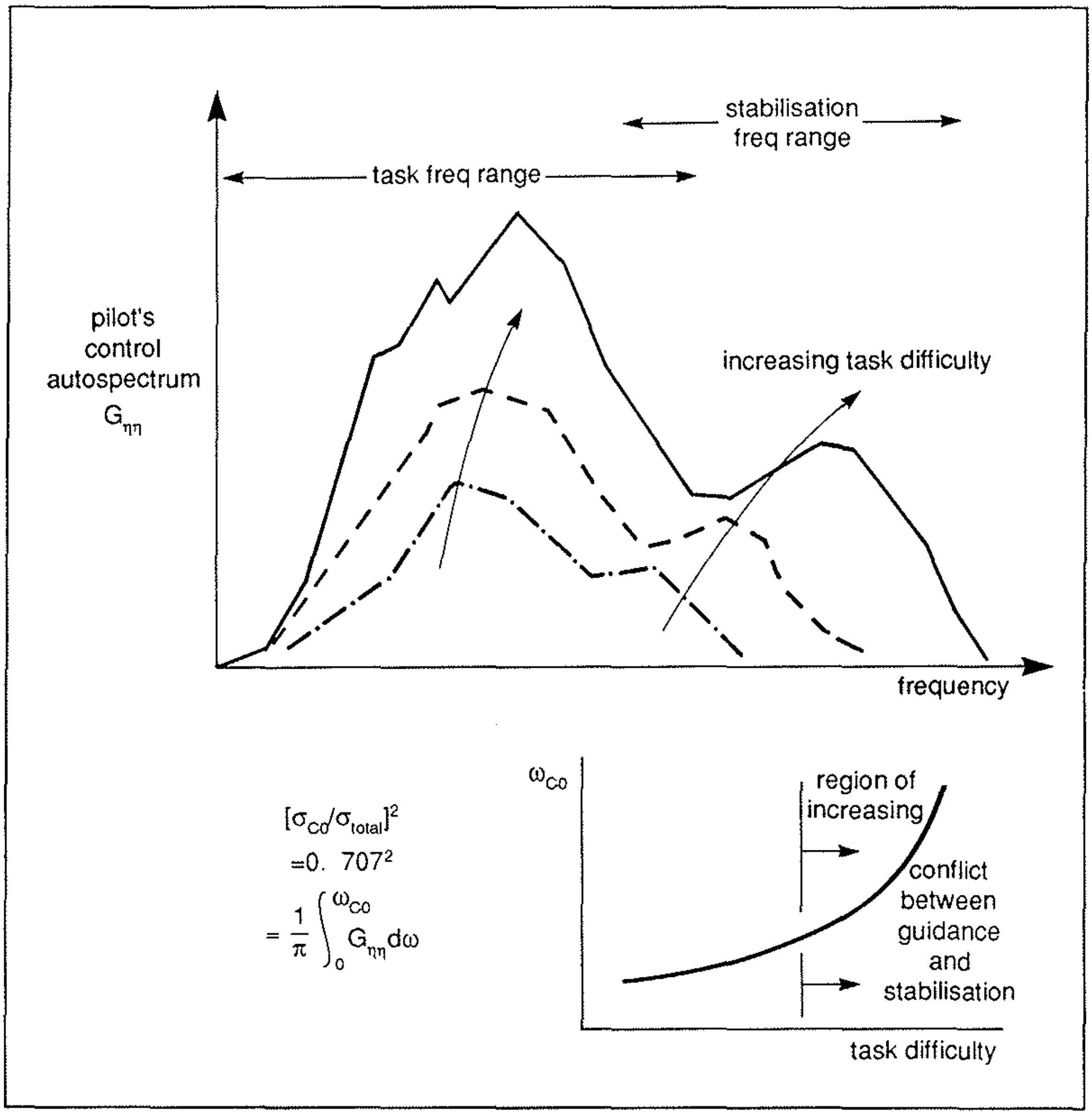

Fig 1 Conceptual Relationship Between Pilot Cut-Off Frequency and Task Difficulty

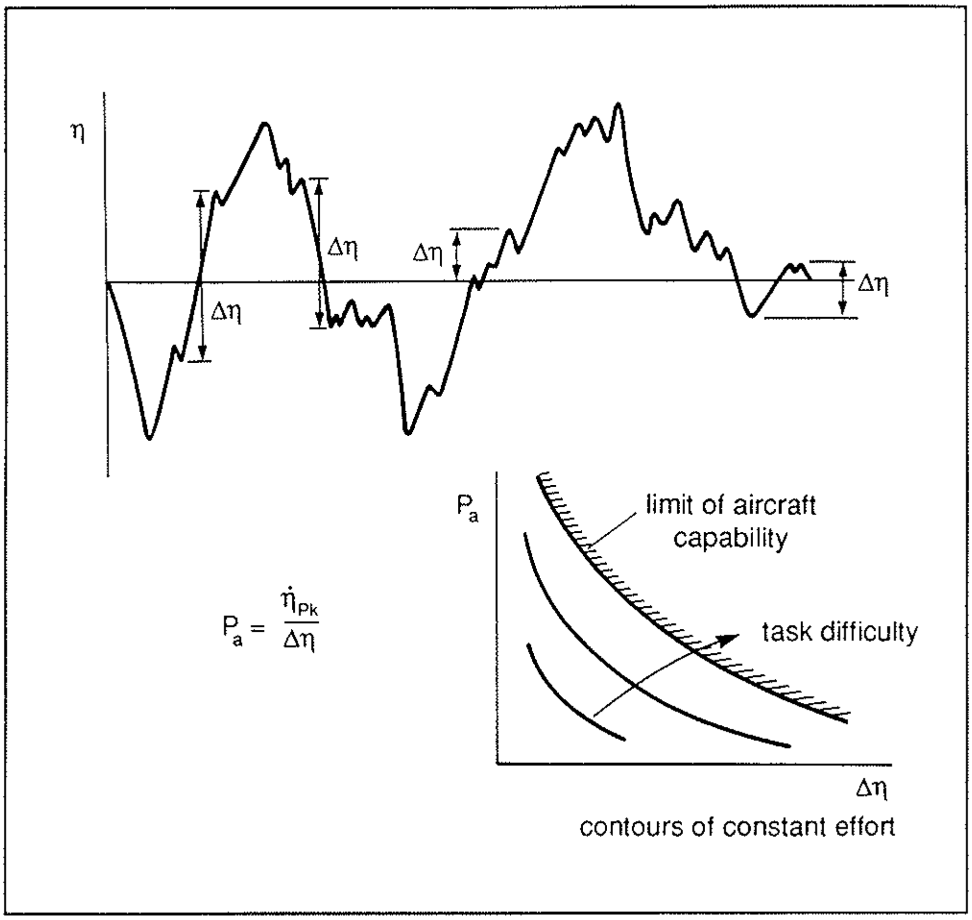

Fig 2 Conceptual Relationship Between Pilot Attack and Task Difficulty

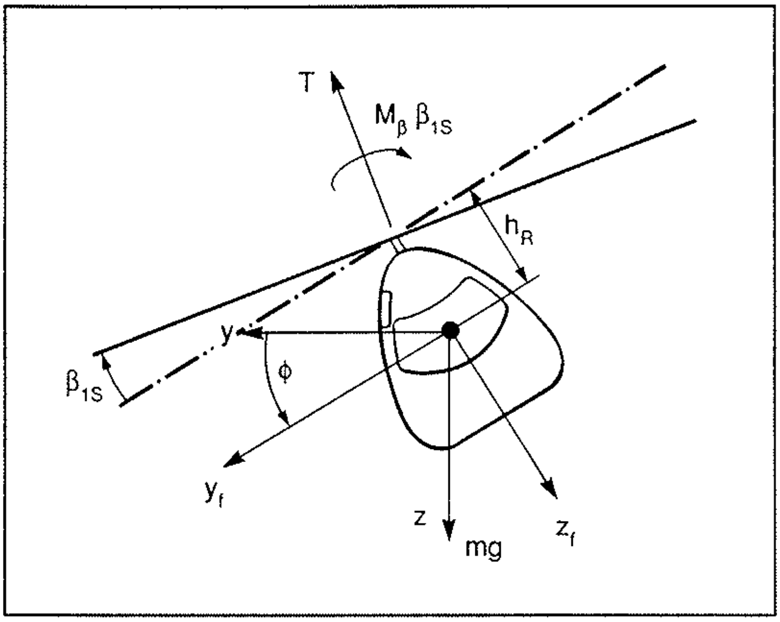

Fig 3 Helicopter Force Balance in Lateral Manoeuvres

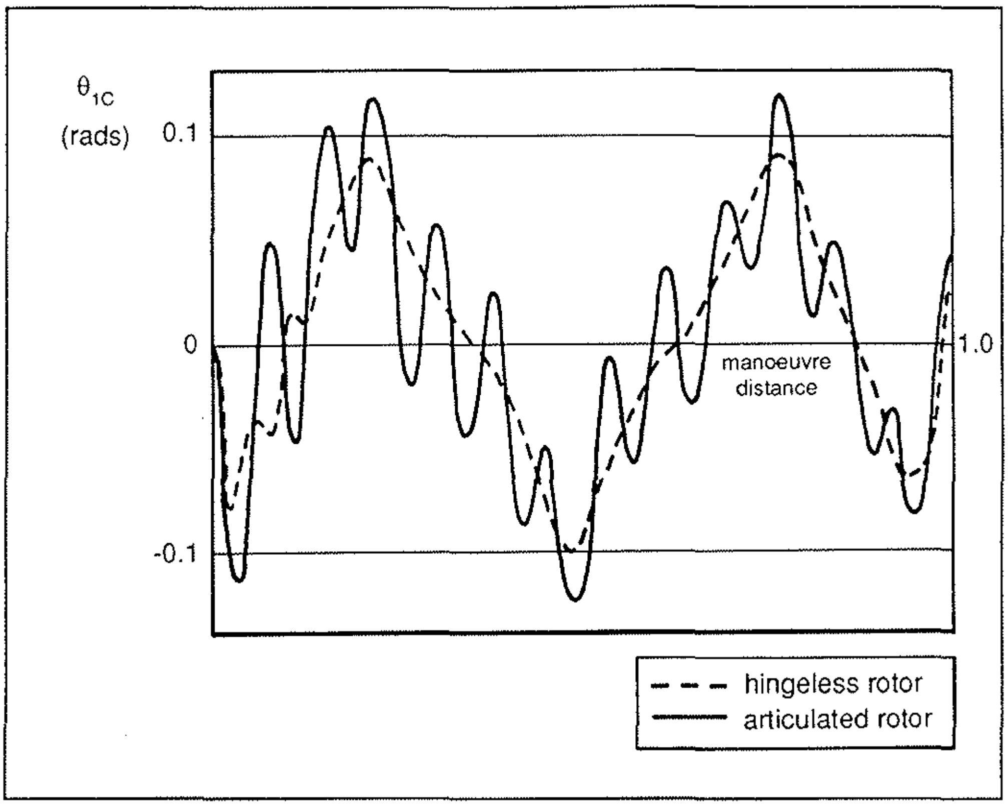

Fig 4 Comparison of Lateral Cyclic Required to Fly a Lateral Slalom from Simple Theory

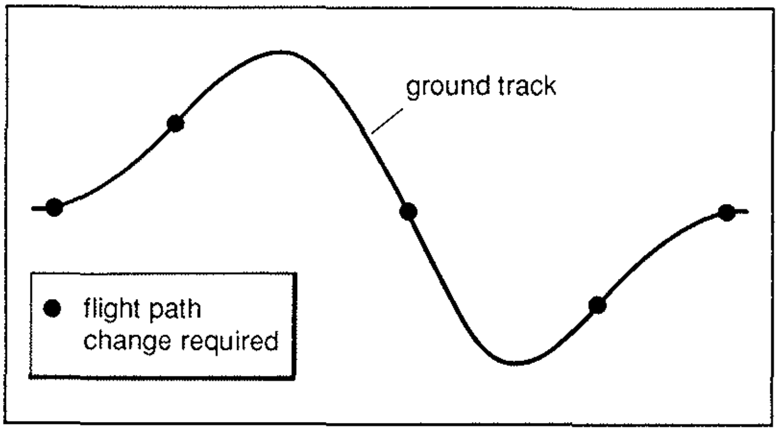

Fig 5 Flight Path Changes in Two-Sided Slalom

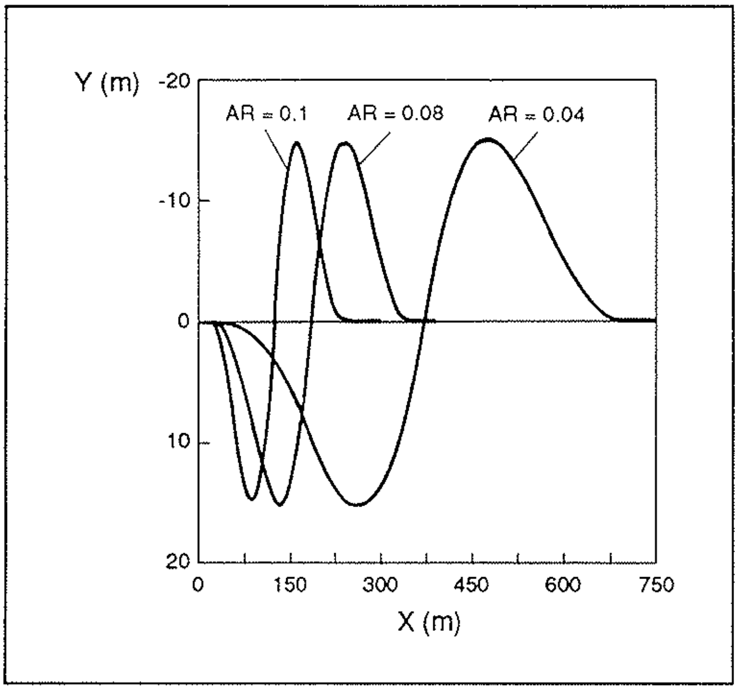

Fig 6 Helinv Version of the ADS33C Slalom

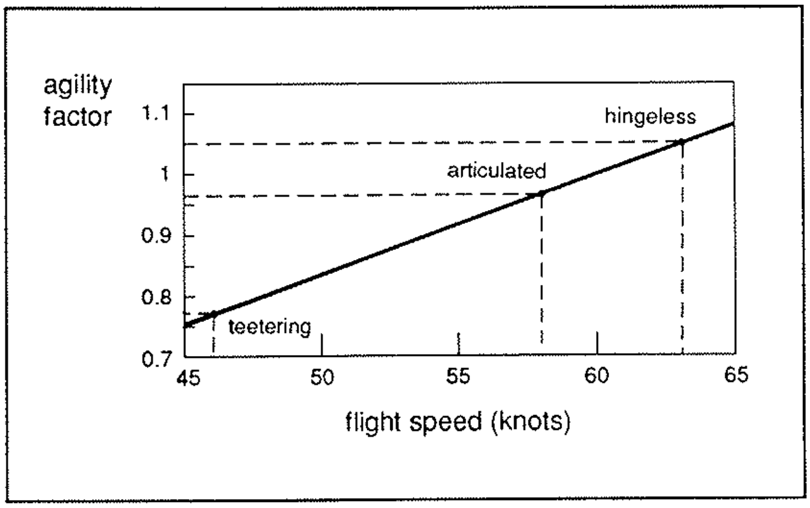

Fig 7 Maximum Agility Factors for Lynx with Different Rotors as a Function of Flight Speed

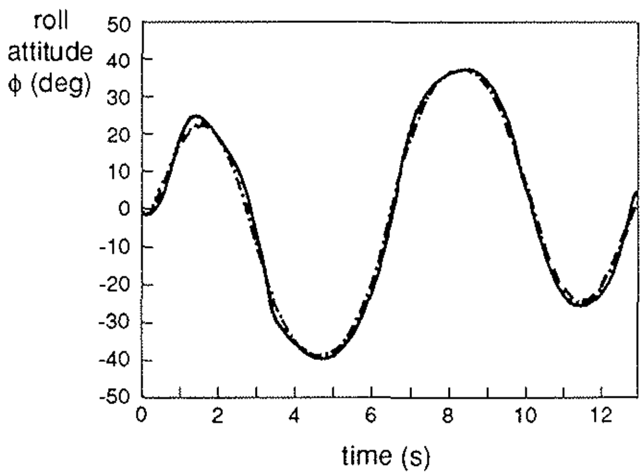

(a) Roll attitude variations

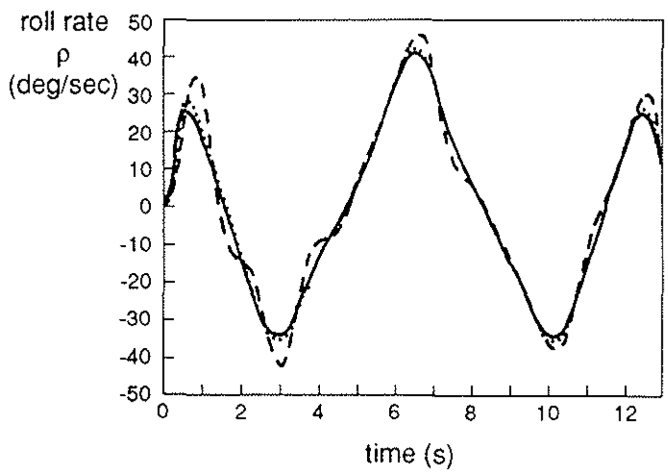

(b) Roll rate variations

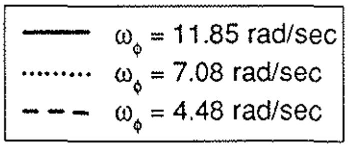

Fig 8 Roll Attitude and Rate as a Function of Manoeuvre Time for Lynx with Different Rotors Flying the AR = 0.077 Slalom

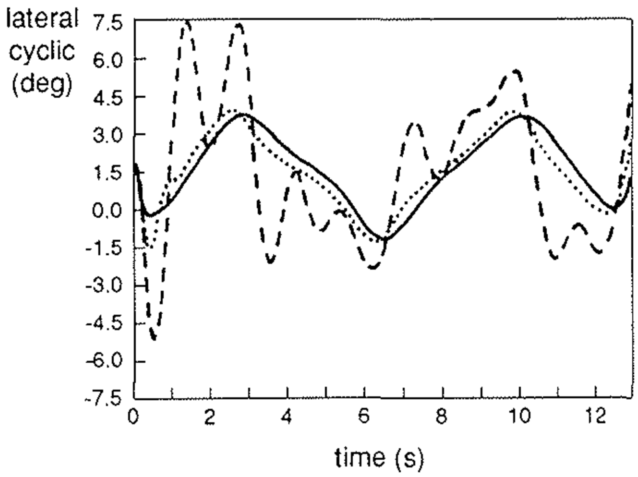

(a) Lateral cyclic time histories

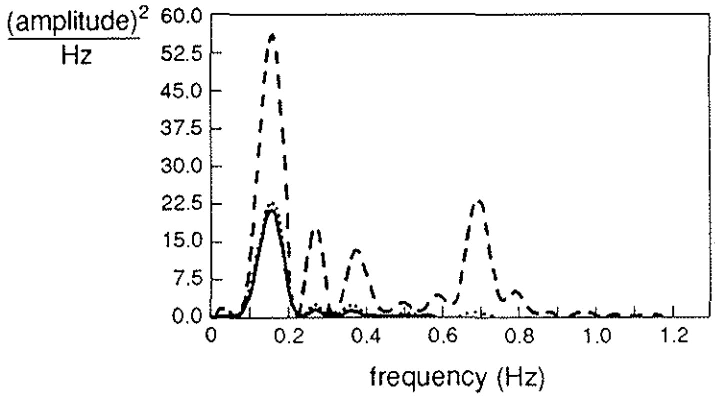

(b) Lateral cyclic autospectrum

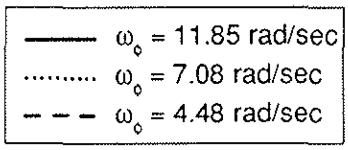

Fig 9 Lateral Cyclic Control Activity for Lynx With Different Rotors Flying the AR = 0.077 Slalom

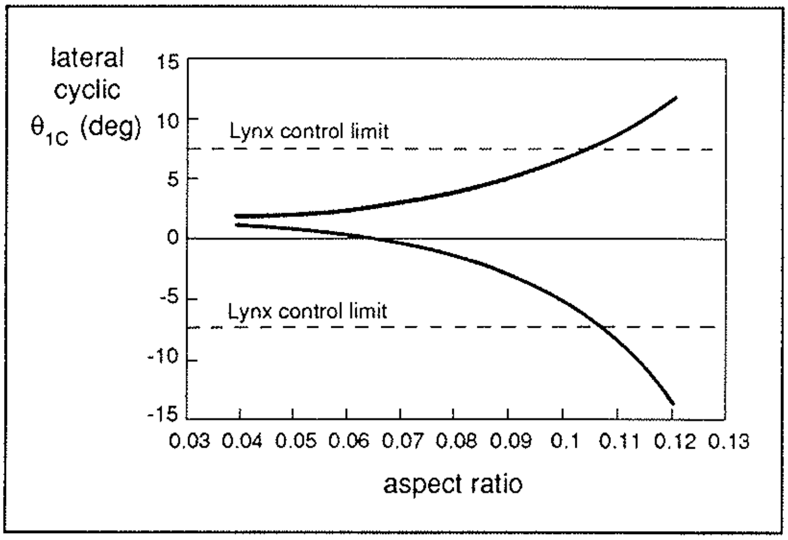

Fig 10 Maximum Cyclic Used By Lynx Flying Slalom as a Function of AR

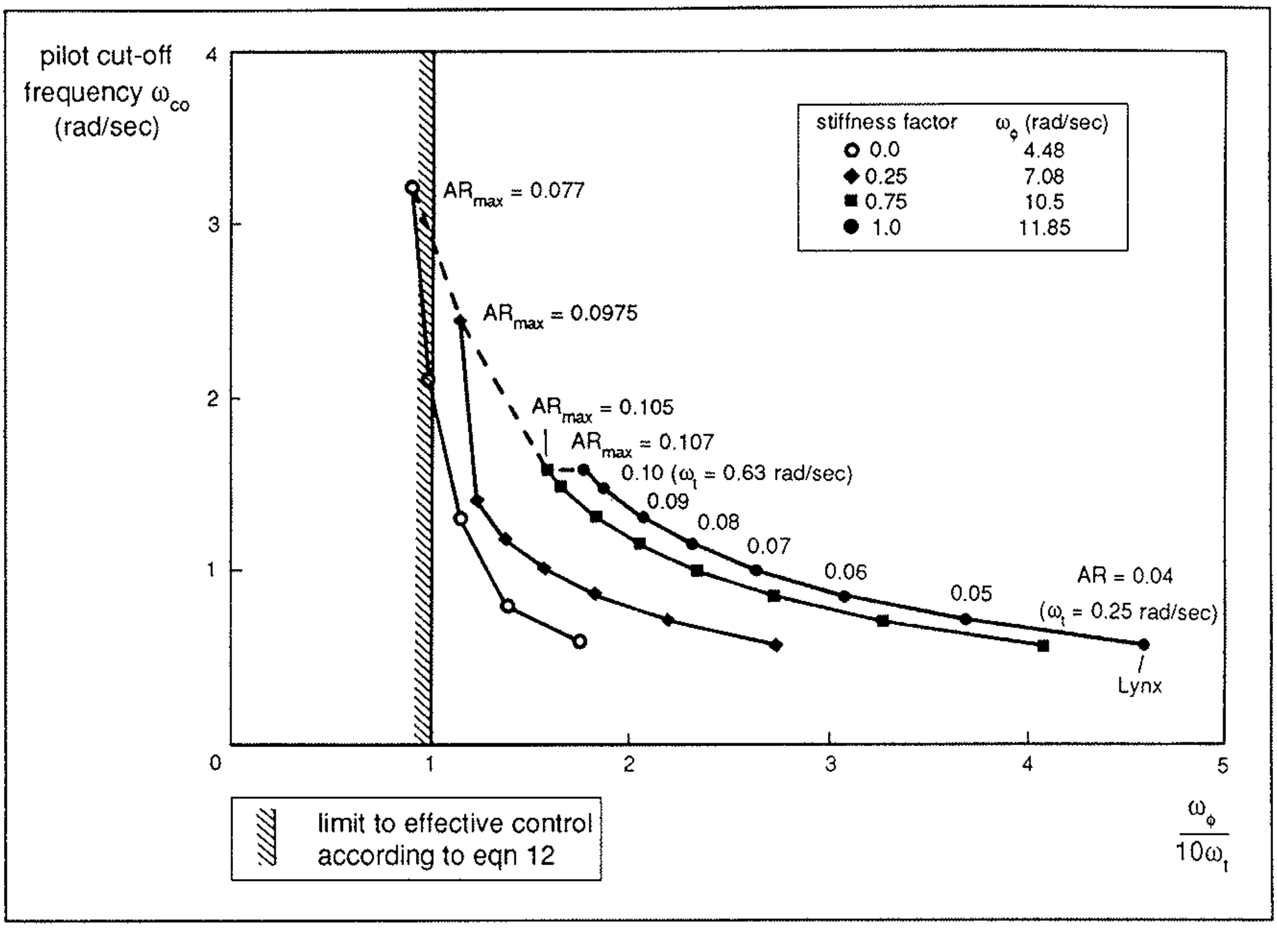

Fig 11 Pilot Cut-Off Frequency as a Function of Frequency Ratio ω_ϕ/ω_t For HELINV Slalom Flights

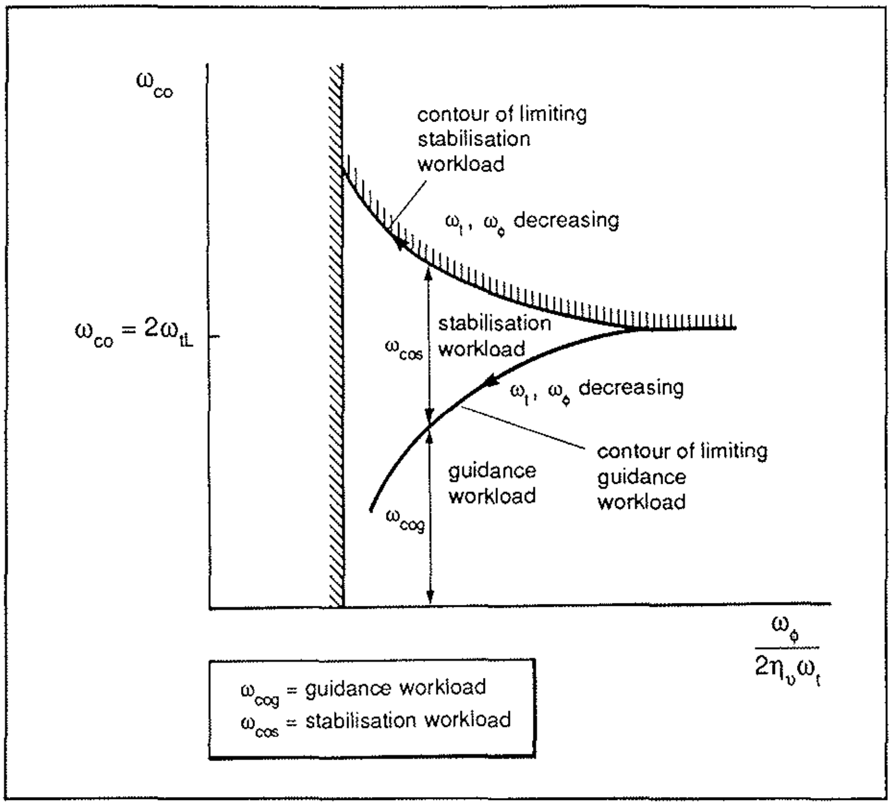

Fig 12 Conceptual Relationship Between Pilot Cut-Off Frequency and Bandwidth Ratio

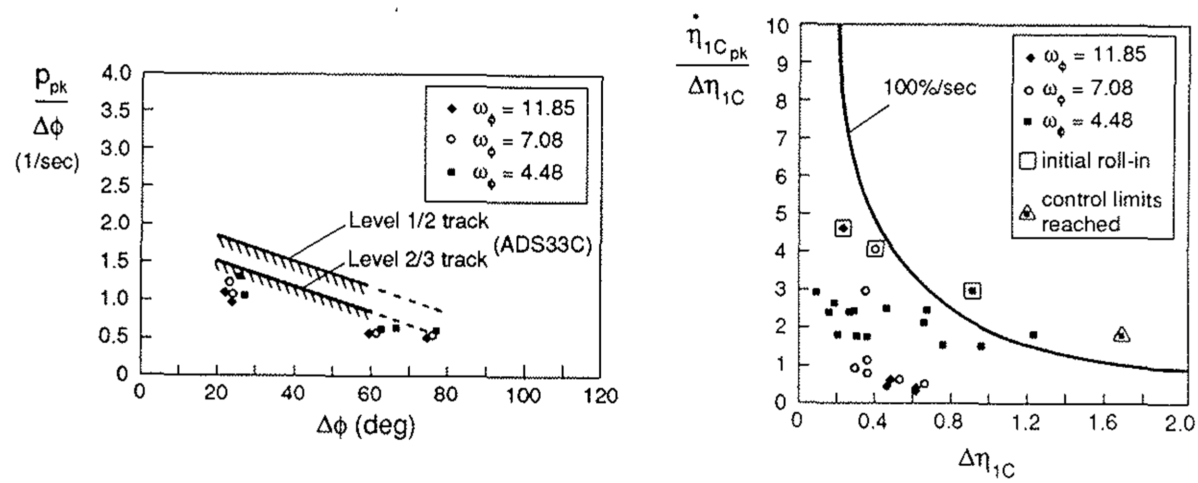

(a) Roll Attitude Quickness Chart

(b) Lateral Cyclic Attack Chart

Fig 13 Transient Response Characteristics For HELINV Slalom Flights

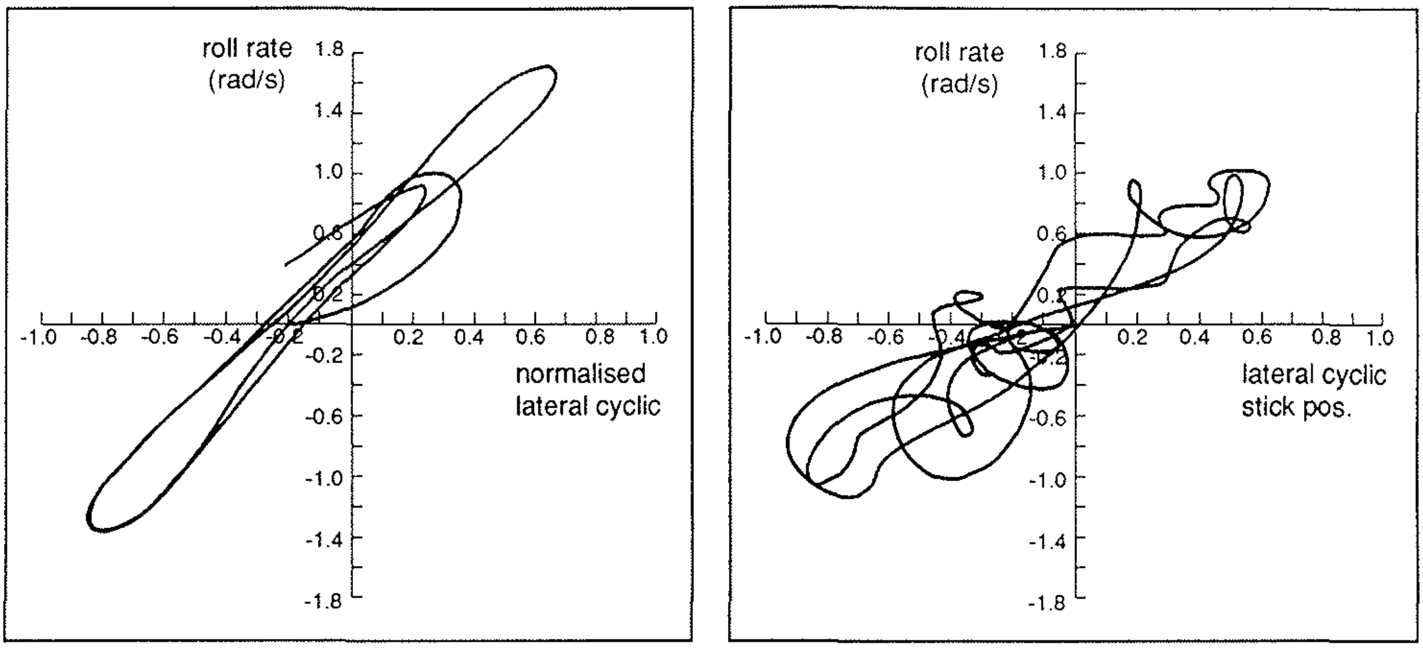

(a) Helinv

(b) Flight test

Fig 14 Cross Plot of Lynx Lateral Cyclic Against Roll Rate in the Slalom

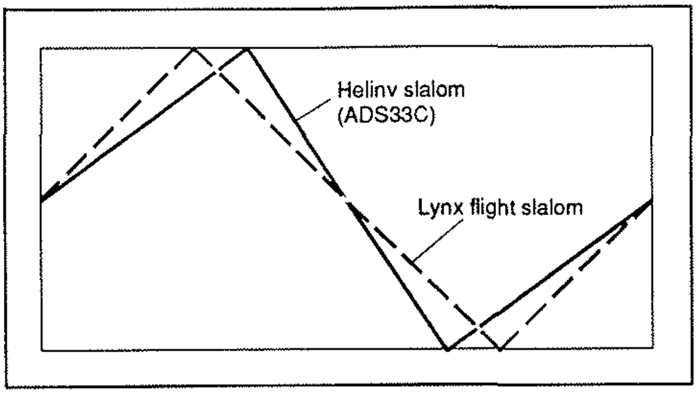

Fig 15 Comparative Layout of Helinv and Flight Slaloms

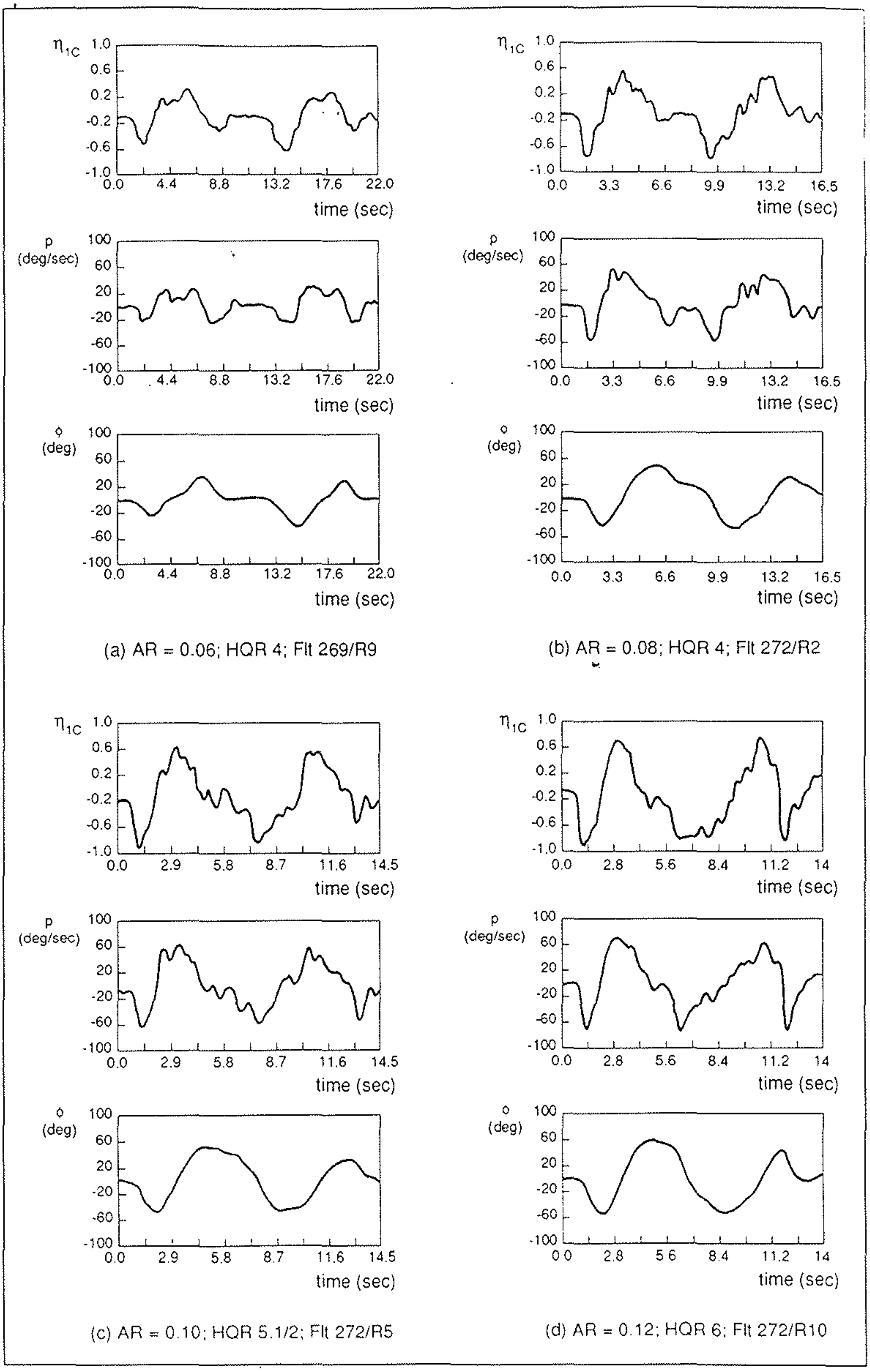

(a) AR = 0.06; HQR 4; Flt 269/R9

(b) AR = 0.08; HQR 4; Flt 272/R2

(c) AR = 0.10; HQR 5.1/2; Flt 272/R5

(d) AR = 0.12; HQR 6; Flt 272/R10

Fig 16 Flight Results for ALYCAT Lynx Flying Slaloms

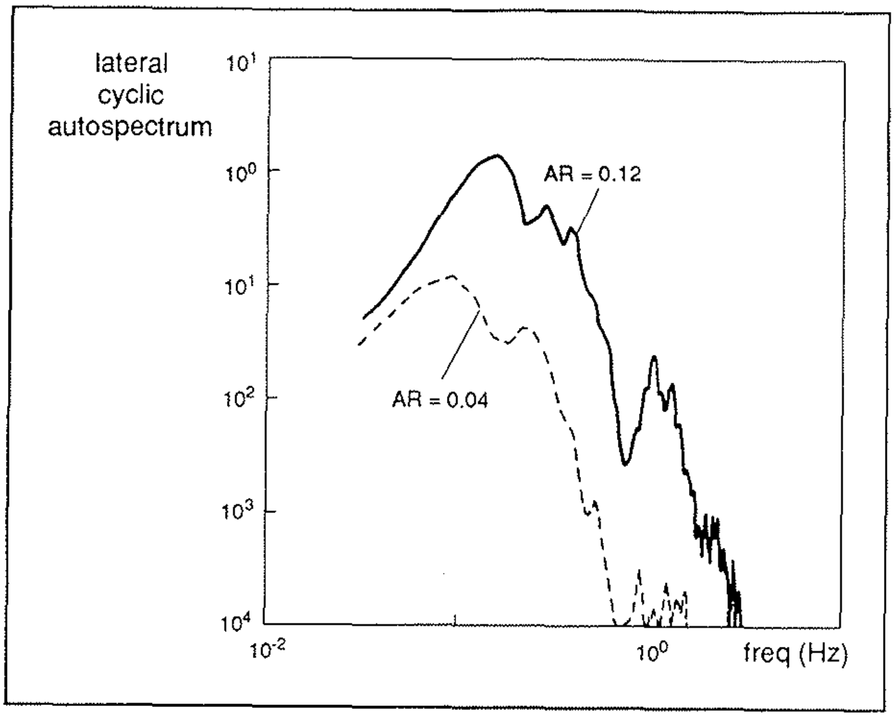

Fig 17 Lateral Cyclic Auto spectrum For Lynx Flying Slaloms

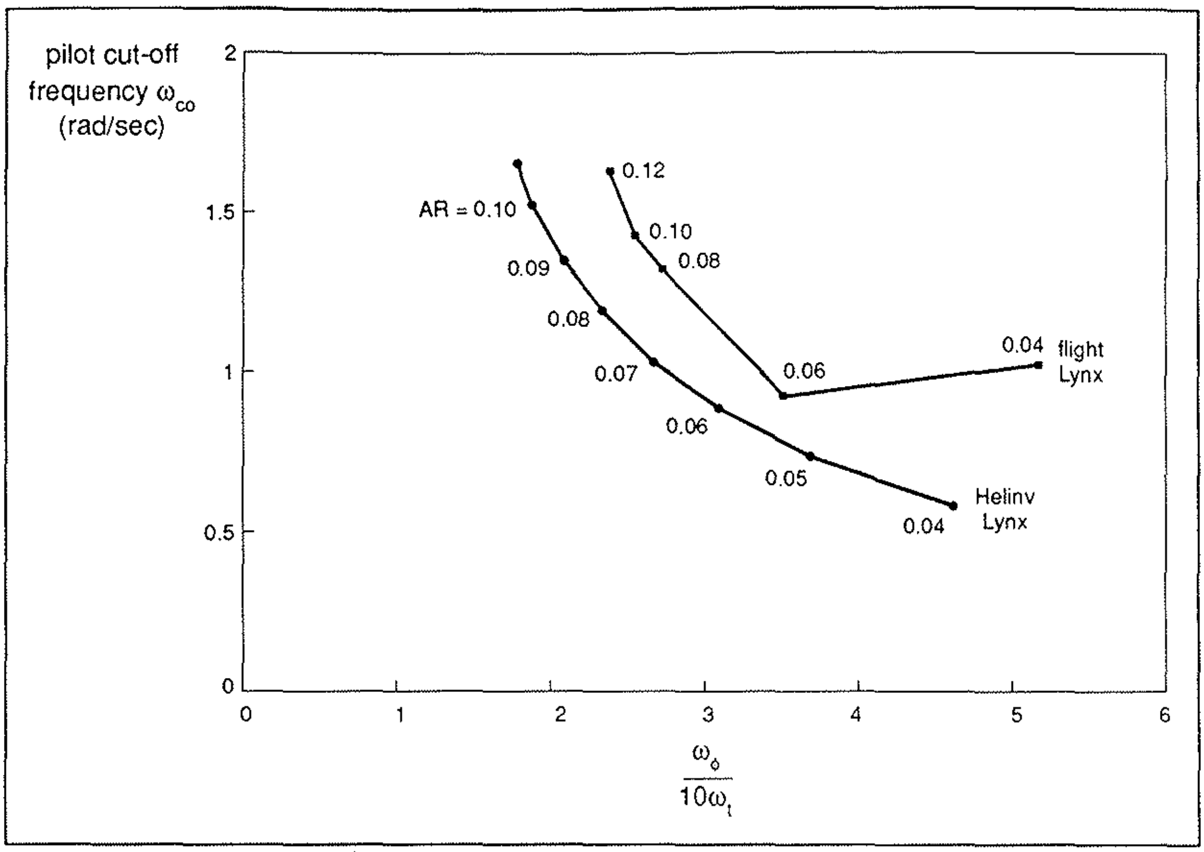

Fig 18 Comparison of Pilot Cut-Off Frequency For Lynx - Flight vs HELINV

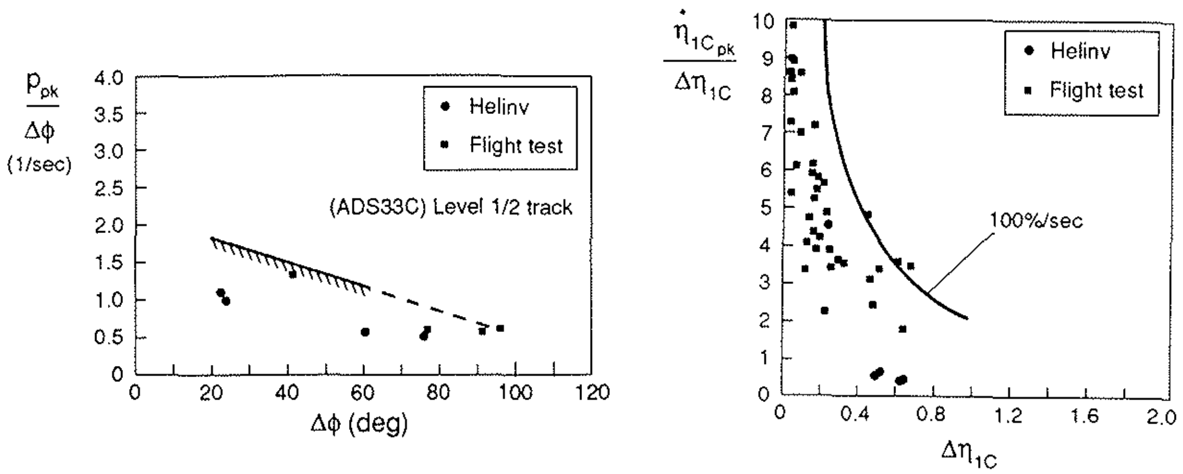

(a) Attitude Quickness

(b) Lateral Cyclic Attack

Fig 19 Transient Response Properties of Lynx Flight Slalom Results (AR = 0.08)

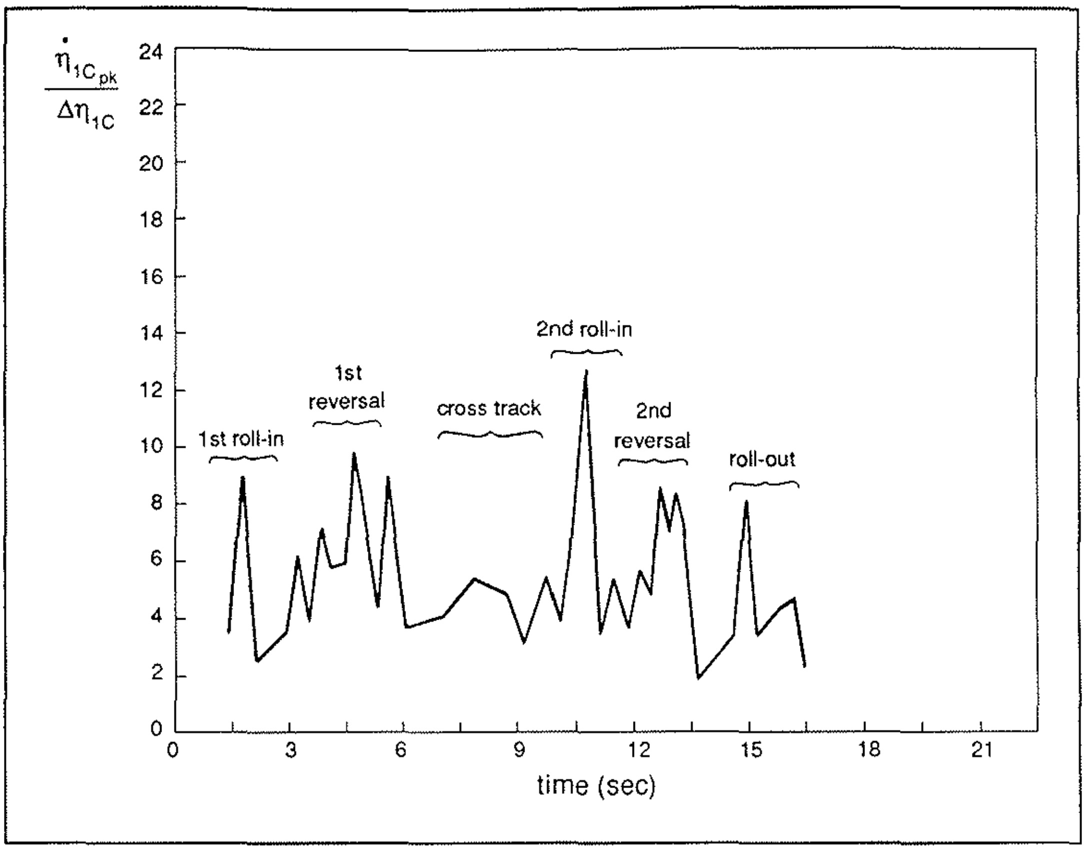

Fig 20 Temporal Variations of Cyclic Attack in the Slalom (AR = 0.08)

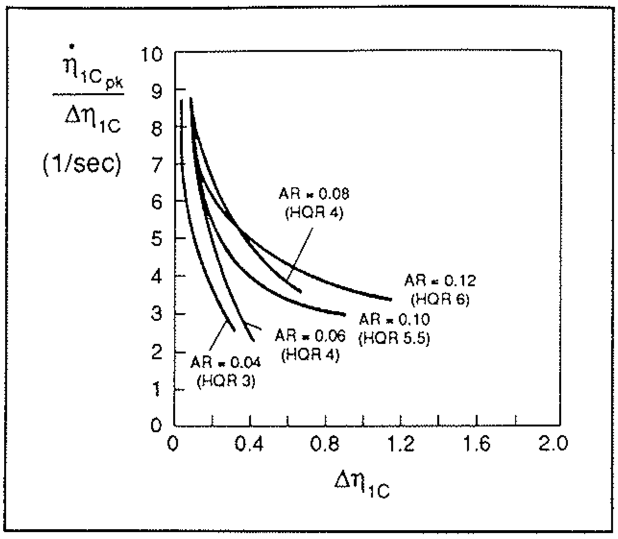

Fig 21 Lateral Cyclic Attack Boundaries For Lynx Flying Slalom

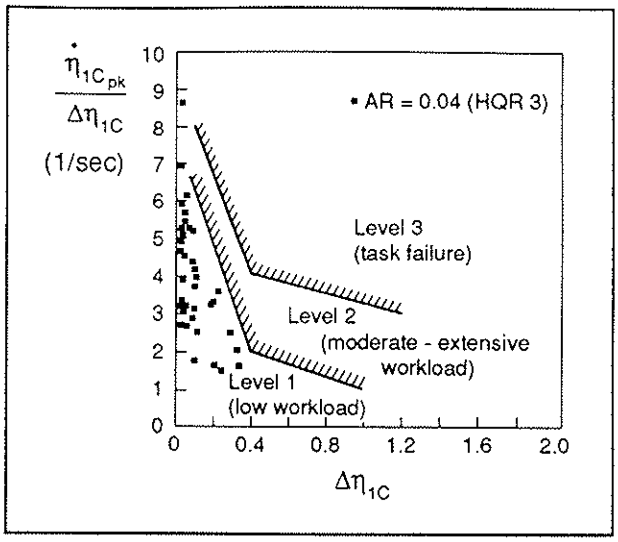

Fig 22 Tentative Workload Boundaries on Attack Chart

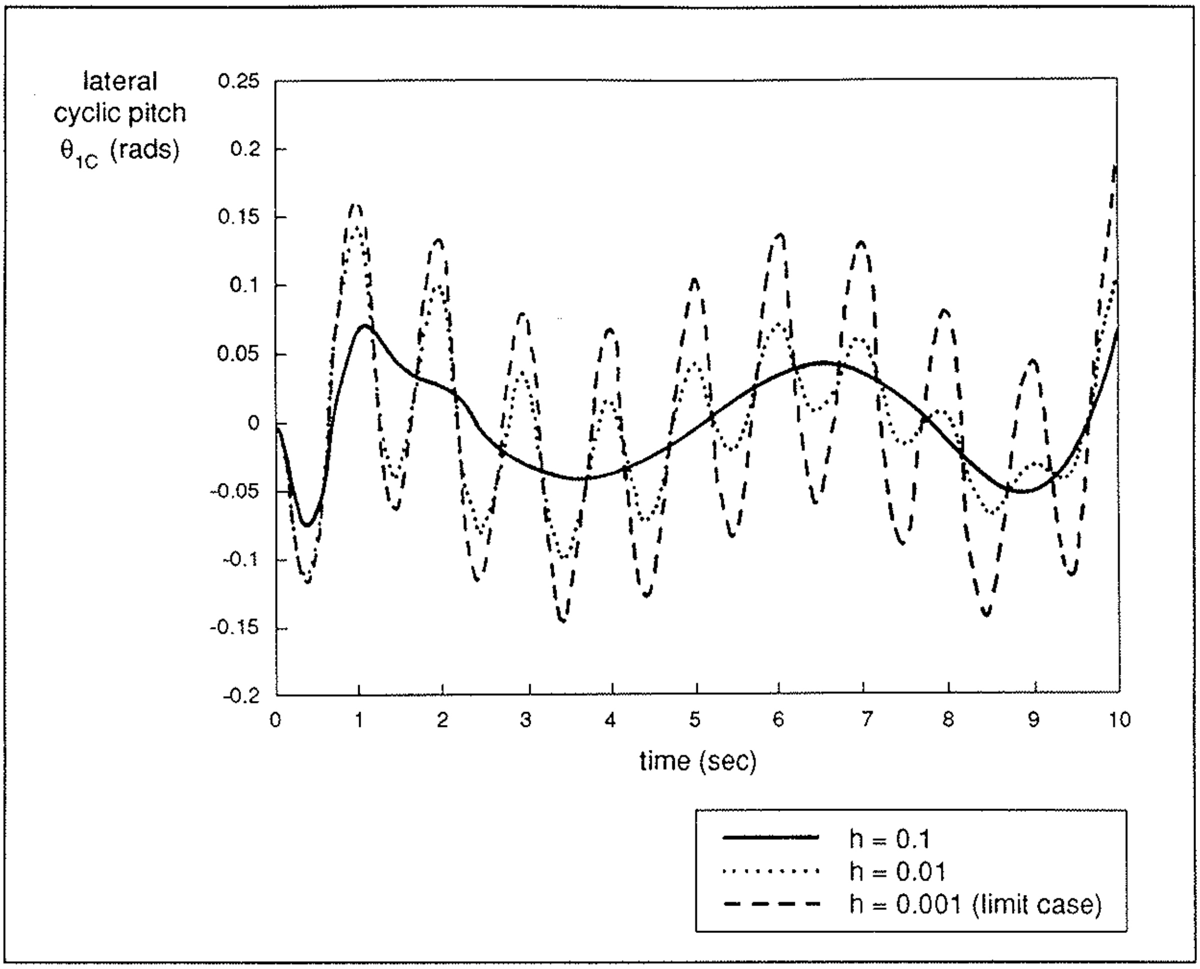

Fig A1 Effect of Integration Time-Step on Level of Damping in Roll Oscillation